Discrete Windowed-Energy Variable Structure Passivity Signature Control for Physical Human-(Tele)Robot Interaction

Smrithi Thudi and S. Farokh Atashzar, *Member, IEEE*

***Abstract*—In this letter, we propose a novel adaptive iterative stabilization method for physical human-(tele)robot interaction, named Discrete Windowed-Energy Variable Structure Passivity Signature Control (DWE-VSPSC). The proposed stabilizer is capable of adaptively translating the knowledge domain regarding the capacity of the user's biomechanics in absorbing physical interaction energy to reduce the transparency distortion (induced for stabilization) while enhancing system performance through a flexible design of stabilizer. The contributions of this letter are: (1) the design of a novel discrete adaptive stabilizer with proof of stability; allowing for digital implementation of the intelligent algorithm; (2) introducing the concept of "windowed energy stabilization" for the proposed variable structure passivity-signature controller in order to allow for tuning the energy behavior of the interconnected system while making a balance between conservatism and agility of the system; (3) relaxing any assumption on the passivity behavior of the environment while being able to handle stochastic variable network delays without any restriction on the rate of change of delay or the delay. The mathematical design of the stabilizer is provided alongside the stability proof. Also, the performance of the system is evaluated using a systematically-designed grid simulation study for a large range of delay and environmental impedances ranging from passive to non-passive behaviors. A direct application of the outcome is for telerobotic rehabilitation and telerobotic surgery.**

***Index Terms*—Haptics, physical human-robot interaction, variable structure passivity control, telerobotics.**

I. Introduction

ONE of the main challenges of telerobotic and human-centered robotic systems is the stability and reliability in the presence of force feedback. This topic is critically important for in-home delivery of care (such as telerobotic rehabilitation). Communication delay and variability in the delay can result in the accumulation of interaction energy in the loop of interaction and can significantly degrade the stability [1]. Several techniques have been proposed for the stability of bilateral teleoperation systems with time delay. Small-gain theory [2] and passivity control theory [3]–[5] make the foundations of most of the existing techniques (please see our research on this topic: [6]–[9]). Two reputable conventional passivity stabilizers are Wave Variable Control [10] and Time Domain Passivity Approach (TDPA) [11], [12]. Variations of passivity based approaches have been extensively investigated in the literature (e.g., [13]–[17]).

Despite the strong performance, most existing stabilizers assume the environment to be passive, rejecting any non-passive energy/power delivery, which sometimes encodes information regarding the type of task to be conducted (such as assistive behavior of a therapist using telerobotic rehabilitation or assistive force field in exoskeletons). The assistive behaviors of a robot and delivery of assistance through a telerobot are equivalent to the injection of energy. Thus, in many cases besides the conventional sources of non-passivity, i.e., communication delay and changes in delays, there is a third source of non-passivity, the effect of which should not be completely compensated. Thus new applications of telerobotic and human-centered robotic systems call for new stabilization schemes that are flexible with various characteristics of the task and compatible with non-passive environments while reducing the conservatism and complexity.

In some cases, conventional controllers result in additional loops (to inject damping), the implementation of which can practically complicate the topology of the control and result in unexpected behaviors [6], [8]. In addition, using conventional passivity-based approaches, the effect of the user's biomechanics is not considered, resulting in the excessive injection of damping even when the system would not be unstable due to the inherent natural damping of the user's biomechanics.

To address the issues above, we have recently investigated the quantifiable energetic behavior of human limb to design a new family of stabilizers [6], [8]. We have adopted the concept of the excess of passivity (EoP) from the "Strong Passivity Theorem (SPT)." EoP quantifies the energetic margin, which can be exploited to guarantee the stability of the system while allowing for non-passive energy to flow without damaging the transparency that is critical in assistive robotics. The experimental setup and some of our preliminary results [6], [8] on passivity maps are shown in Fig. 2.

In this letter, we propose a novel stabilizer related to the concept of the EoP in human biomechanics for use in safe human-robot interaction. The paper has three main novel contributions:

Manuscript received October 15, 2020; accepted February 24, 2021. Date of publication March 8, 2021; date of current version March 25, 2021. This letter was recommended for publication by Associate Editor K. Hashtrudi-Zaad and Editor J-H Ryu upon evaluation of the reviewers' comments. This study was supported in part by the startup fund from NYU granted to Atashzar, and in part by the National Science Foundation (Awards: # 2037878, and # 2031594).
(Corresponding author: S. Farokh Atashzar.)

Smrithi Thudi is with the Department of Mechanical and Aerospace Engineering, New York University (NYU), Brooklyn, NY 11201 USA (e-mail: smrithi.reddy.14@gmail.com).

S. Farokh Atashzar is with the Department of Mechanical and Aerospace Engineering, New York University (NYU), Brooklyn, NY 11201 USA and also with Department of Electrical and Computer Engineering, NYU, and is affiliated with NYU WIRELESS, and NYU Center for Urban Science and Progress (CUSP) , NY 11201 USA (e-mail: f.atashzar@nyu.edu).
Digital Object Identifier 10.1109/LRA.2021.3064204

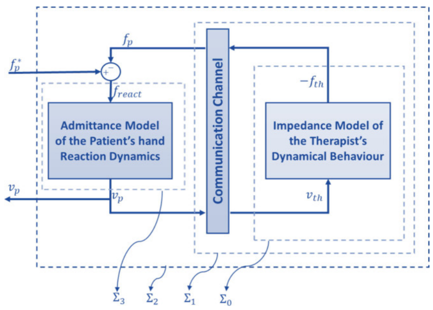

Fig. 1. Interaction of the admittance of the patient's reactive biomechanics with the impedance of the therapist's behavior.

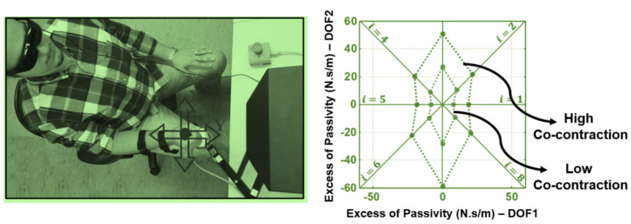

Fig. 2. Experimental setup and result based on our previous work [6], showing the changes in EoP for 2 degrees of freedom and the effects of the co-contraction.

(1) we propose a novel formulation of discrete-time passivity signature-based stabilization while enabling the exploitation of the knowledge on the user's energetic behavior of the biomechanics and the corresponding changes, (2) instead of using damping loops for stabilization that can result in an increase in complexity, and practical stability problems, we will introduce an adaptive force scaling while removing the dependency to the sampling time (note: dependency to sampling time results in chattering for conventional approaches); (3) We introduce the concept of tunable windowed energy for the proposed variable structure passivity-based stabilization while considering the EoP. The latter allows the operator/designer to tune the energetic conservatism of the system. A novel mathematical formulation of the stabilization framework is developed, and the stability proof is discussed. An extensive grid simulation study is conducted to evaluate the performance of a wide range of time delays and environmental impedances.

II. Preliminaries

Two-channel bilateral leader-follower teleoperation architecture is used in this letter based on the formulation in [9]. Under no communication delay and sources of non-passivity, this architecture is able to achieve maximum transparency while reducing the artifacts of uncertainties and unmodeled dynamics, which may cause waveform distortion for modalities of interaction [2], [18]. In this letter, we relax the assumption of passivity on the (physical and virtual) environment side, and we also relax the conventional assumption of linearity on both the environment side and the operator side. The paper is developed considering the telerehabilitation application.

In this context, using the two-channel architecture, the motion trajectories of the patient on the leader robot is transmitted across the communication channel and replicated for the therapist at the follower side so that the therapist can react by generating assistive/resistive forces, which will be transmitted back and replicated by the leader robot for the patient. Thus, the interaction loop is closed over the communication network, which may show stochastic jitter and unknown time-variable latency's, resulting in time-varying behavior (more details in [8]). The resulting interactional loop is shown in Fig. 1. Under ideal delay-free conditions and when the stabilizer is not activated to modify the energy, we have

$$f_p = \hat{f}_{th}, \;\; and \;\; v_{th} \;\; = \hat{v}_p \tag{1}$$

In (1) f_p is the interaction force applied by the patient to the leader robot. $\hat{f}_{th}$ is the delayed environmental (therapeutic) force received from the therapist/environment at the follower side through the first communication channel. Also, v_{th} is the velocity at the therapist side and $\hat{v}_p$ is the delayed patient's limb velocity transferred across the second communication channel and received at the environment (therapist) side.

The environment can be a remote human therapist in the loop, or a computerized local or cloud-based algorithm, such as in exoskeletons, or it can also be a generic environment.

In Fig. 1, the patient terminal $\sum_3$ is the admittance model of the patient's reaction dynamics. $\sum_0$ is the impedance model of the assistive/resistive therapist terminal. The fusion of the communication channel and the therapist terminal is $\sum_1$, which has all sources of non-passivities, including the time-delay, the variation of the time delay, and the non-passive (e.g., assistive) behavioral dynamics of the therapist.

It should be noted that the patient's side interactional force f_p can be decomposed into (a) an active component that generates motion f_p^* and (b) an inherent reactive component f_{react} that is the repulsive inherent biomechanical response which generates resistance in response to spontaneous robot's motion (f_{react} changes by the co-contraction of the muscles).

$$f_p(t) = f_p^*(t) - f_{react}(t), \text{ where } f_{react}(t) = z_p(v_p, t) \tag{2}$$

In (2), $z_p(v_p, t)$ is a non-autonomous nonlinear impeding dynamical behavior of the biomechanics. This model relaxes the linearity assumption. To summarize, this work relaxes the conventional restrictive assumptions as summarized in the following: • This letter considers nonlinear and non-passive therapy terminal. Although the therapy terminal may represent passive behavior during resistive tasks (needed for later stages of rehabilitation), it can also strictly represent non-passive behavior, such as during assistive therapy when the human therapist or wearable exoskeleton induce mechanical energy into the system to empower the user. • This letter considers stochastic non-passive time-varying time delays for the communication network without imposing any conventional restrictive assumptions on the rate of change of delay or the maximum delay. • This letter allows for non-autonomous and nonlinear biomechanics of the patient in absorbing the mechanical energy; thus, conventional assumptions on linearity and time-invariant behaviors (such as classical linear mass-spring-damper models) are relaxed. Based on our prior research on human upper-/lower-limb biomechanics [6], [19] we know that the dynamics are dissipative; thus, a positive EoP can be considered. The EoP may be changing in value due to the muscle co-contraction levels. The mathematical framework of this paper is flexible and can also take hypothetically non-passive reactive dynamics for the patient's biomechanics.

A. Passivity-Based Foundations

Based on the strong passivity theory [20], [21], the two-channel loop shown in Fig. 1 is stable if the interconnection $\sum_2$ is passive. Although the therapist (the environment) and the communication may not be passive, the entire system can still remain passive if the impeding-component of the patient's biomechanics can absorb the energies injected by the non-passive therapy terminal (environment + communication). If the biomechanics is not able to compensate, then a control action must be activated to stabilize the. This is the logic of the proposed stabilizer. To design such a controller (see Section III), two definitions for system passivity should be reviewed. For a system with input vector, u_{in}, output vector y_{out}, and initial energy β at t > 0, the system is said to be

1) Passive, if $\forall$ t ≥ 0 $\exists$ a constant β such that

$$\int_0^t u_{in}(\tau)^T.y_{out}(\tau)d\tau \geq \beta \tag{3}$$

2) Output Strictly Passive/Non-Passive, if $\forall$ t ≥ 0 $\exists$ a constant β such that

$$\int_0^t u_{in}(\tau)^T.y_{out}(\tau)d\tau \geq \beta + \xi.\int_0^t y_{out}(\tau)^T.y_{out}(\tau)d\tau, \tag{4}$$

when $\xi \geq 0$ then the system is Output Strictly Passive (OSP) with EOP of ξ. If $\delta < 0$ then the system is Output Non Passive (ONP) with SOP of ξ.

Strictly passive systems are asymptotically stable. An OSP system is L2 stable with finite L2 gain $\leq 1/\xi$ where ξ is the EOP of the OSP system [22].

B. Estimation of EoP

The biomechanical EoP is the inherent ability of the limb biomechanics in absorbing the interaction energy. Biomechanical EoP works like an energy reservoir. In the last five years, we have generated the mathematical foundations to estimate this biological capacitance as we believe it can be used to design a family of intelligent stabilizers that can evaluate the available energetic resources and modulate the flow of non-passive power/energy accordingly. We have designed a preliminary stabilizer through the extension of TDPA [6], [8] to take into account some constant conservative estimation of biomechanical EoP to form a nonlinear lower bound on the energetic behavior of human biomechanics.

However, in practice, EoP is a variable parameter that changes due to several factors, including healthy voluntary co-contraction. Even stroke itself can cause higher muscle tone, fatigue, joint laxity, involuntary movements, and abnormal muscle stiffness [23], all of which can affect the EoP.

To utilize the biomechanical EOP in the design of a controller, a real-time estimation is required during interaction with the robot. For this, Atashzar *et al.* have established a systematic procedure for the upper limb [6] and recently for decoding the passivity of the hip joint [19].

To summarize, the procedure has two steps, (a) offline EoP identification, (b) online EoP extrapolation and tracking. For offline identification in our previous work [6], the users were asked to isometrically grasp the haptic device (but not kinesthetically fixate the position) prior to operation. This was done once with a rigid grasp (high co-contraction) and once with a soft grasp, while no exogenous kinesthetic forces are applied in both cases, and hence $f_p^* \to 0$. Therefore, $f_{react} = -f_p$, since $f_p^* = f_{react} + f_p$ (from the Fig. 1). Both f_p and v_p are measured. The robot then applies sinusoidal, linear, and angular participants to the arms and wrists with frequencies ranging from 0 to 2 Hz. In order to account for the directionality of the EoP map, the biomechanics were perturbed in 8 directions ranging from 0 to 2π. This allowed to generate a directional pre-operative map of EoP and to also decode the effect of muscle contraction (details about the performance can be found in [6], [9]). Our preliminary studies showed the possibility of kinematics-related changes which is possible to study (since the users are holding the robots) to further enhance the performance; however, in the context of rehabilitation, the workspace is quite limited, and our preliminary work did not suggest a major change in EoP caused by kinematics (however, more in-depth analysis of the effect of kinematics is a direction of future research).

An example of the resulting EoP map is shown in Fig. 2, in which the smaller contour shows EoP for the low level of contraction and the larger contour shows the EoP for the high level of contraction. The EoP map correlates the EoP to the geometry of interaction and the co-contraction level. Both of these parameters can be measured in real-time to give an online extrapolation of EoP, based on real-time data, to be used by the stabilizer.

It should be noted that (based on the design of the stabilizer, explained later) any estimate of EoP, even the most conservative one when incorporated into the stabilizer, will result in better performance when compared with state-of-the-art TDPA (since existing methods completely ignore energy absorption by biomechanics).

In terms of the mathematical formulation to identify the EoP (through experimental data collection), it can be mentioned that considering zero initial energy for the system (i.e., $\beta = 0$) and OSP model (4), for patient terminal, we have:

$$\int_0^t f_{react}(\tau)^T.v_p(\tau)d\tau \geq \xi_p.\int_0^t v_p(\tau)^T.v_p(\tau)d\tau. \tag{5}$$

From 5, the EoP in i^{th} direction is,

$$\xi_{p-i} = \frac{\int_{Ts_i}^{Te_i} f_{react}(\tau)^T.v_p(\tau)d\tau}{\int_{Ts_i}^{Te_i} v_p(\tau)^T.v_p(\tau)d\tau}, \tag{6}$$

where, ξ_{p-i} is the EoP, and Ts_i, and Te_i are the starting and ending time of the perturbation in the i^{th} direction.

III. Method

A. Discrete Windowed-Energy VSPSC (DWE-VSPSC)

In this section, we will introduce the discrete design of the variable structure passivity signature control in the energy domain for the first time and will also extend the design to take into account the windowed energy concept. It can be mentioned that the interconnected system is stable if $\sum_2$, shown in Fig. 1, is passive. This means that

$$\int_0^t f_p^*(\tau)^T.v_p(\tau)d\tau \geq 0. \tag{7}$$

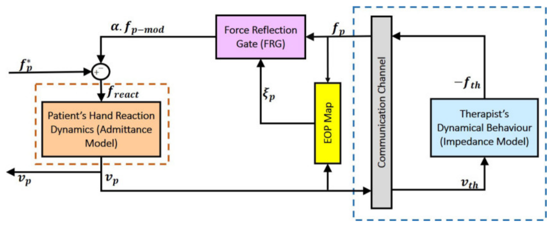

Fig. 3. Discrete Windowed Energy VSPSC.

Considering (7) and the force decomposition (2), the passivity condition of the negative interconnected systems is:

$$\int_0^t f_{react}(\tau)^T.v_p(\tau)d\tau + \int_0^t f_p(\tau)^T.v_p(\tau)d\tau \geq 0 \quad (8)$$

Based on (8) and the flow shown in Fig. 1, it can be seen that the non-passive behavior of the therapy terminal can be compensated for by the passivity of the reactive dynamics of the patient's biomechanics. However, this stability condition may not hold due to a high SoP in the second terminal (caused by delay, and other active behaviors in the system) or low EoP of the biomechanics. Thus a stabilizer should be introduced in a way that guarantees the validity of stability condition at all times.

Here we propose an adaptive force scaling solution for the design of the DWE-VSPSC, the schematic of which can be seen in Fig. 3. The stabilizer is considered to modulate the energy exchange on the fly using the adaptive gain of γ, applied to the delivered force packets, as given below:

$$\begin{aligned} &\text{Let, } f_{p_{mod}} = \gamma.f_p \\ &f_{R_G} = \alpha.f_{p_{mod}} \end{aligned} \quad (9)$$

In (9), $f_{p_{mod}}$ is the force modified by the stabilizer, α is a tunable design parameter, the default of which is unity, and f_{R_G} is the force delivered to the patient. Here, γ is the adaptive gain, which should be calculated on the fly based on the stability design given in the rest of this paper developed using the passivity condition of the system, taking into account (a) the observable flow of energy in real-time, and (b) the EoP of the patient's biomechanics. As mentioned, α, is theoretically considered to be unity. This parameter is basically a simple positive constant design factor ($0 \leq \alpha \leq 1$) generally considered close to unity in case the designer prefers to impose a more conservative stability margin than the one calculated on the fly by the stabilizer, i.e., γ. The α factor reduces the magnitude of the force reflected from the therapist to the patient and can affect the system transparency if smaller than unity.

Considering the notes above, the passivity condition for the interconnected system combined with the stabilizer can be achieved as:

$$\int_0^t f_{react}(\tau)^T.v_p(\tau)d\tau + \int_0^t f_{p_{mod}}(\tau)^T.v_p(\tau)d\tau \geq 0 \quad (10)$$

Considering (10), the next step is to design $f_{p_{mod}}$ based on the real-time observation to guarantee the passivity and thus the stability of the system. As can be interpreted from (10), designing $f_{p_{mod}}$ would require observation of $\int_0^t f_{react}^T.v_p dt$, which is the exact energy that has been damped by the biomechanics. However, this is not achievable since it depends on the measurement of f_{react} which is not a measurable signal when the user is generating exogenous forces to conduct the task (See (2)). To address this challenge, we will take advantage of the definition of the EoP to estimate the variable lower bound on the energy (instead of the exact energy), which is being damped by the biomechanics. For this, based on the OSP condition (5) for the therapy terminal $\sum_3$, assuming zero initial energy ($\beta = 0$), we have

$$\int_0^t f_{react}(\tau)^T.v_p(\tau)d\tau \geq \int_0^t \xi_p.v_p(\tau)^T.v_p(\tau)d\tau. \quad (11)$$

Equation (11) will provide the estimate needed. Combining (11) and (10), the new passivity condition of the system can be achieved as:

$$\int_0^t \xi_p.v_p(\tau)^T.v_p(\tau)d\tau + \int_0^t f_{p_{mod}}(\tau)^T.v_p(\tau)d\tau \geq 0, \quad (12)$$

Based on (12) the stabilizer can be designed in a way that observes the validity of (12) and modifies the energy flow by introducing γ to compensate for the difference of passivity to guarantee the overall passivity and hence stability. As the next step, to calculate γ, we take advantage of the discrete definition of passivity; thus, equation (12) can be rewritten in the discrete domain as (13).

$$\left(\sum_{k=0}^{n} \xi_p.v_p(k)^T.v_p(k) + \sum_{k=0}^{n} f_{p_{mod}}(k)^T.v_p(k)\right)\Delta T \geq 0. \quad (13)$$

Thus, we can say the system is stable if $\psi \geq 0$ when

$$\psi = \sum_{k=0}^{n} \xi_p.v_p(k)^T.v_p(k) + \sum_{k=0}^{n} f_{p_{mod}}(k)^T.v_p(k) \quad (14)$$

As the next step, ψ can be rewritten as:

$$\begin{aligned} \psi = &\sum_{k=0}^{n} \xi_p.v_p(k)^T.v_p(k) \\ &+ \sum_{k=0}^{n-1} f_{p_{mod}}(k)^T.v_p(k) + f_{p_{mod}}(n)^T.v_p(n) \end{aligned} \quad (15)$$

Now let us define

$$Y(n) = \sum_{k=0}^{n} \xi_p.v_p(k)^T.v_p(k) + \sum_{k=0}^{n-1} f_{p_{mod}}(k)^T.v_p(k) \quad (16)$$

Considering (15) and (16) we have:

$$\psi = Y(n) + f_{p_{mod}}(n)^T.v_p(n) \geq 0. \quad (17)$$

As the next step, (16) can be written in an iterative format as:

$$\begin{aligned} Y(n) = &Y(n-1) + \xi_p.v_p(n)^T.v_p(n) \\ &+ f_{p_{mod}}(n-1)^T.v_p(n-1). \end{aligned} \quad (18)$$

The rest of the stabilization synthesis is specifically designed to propose a generalized discrete VSPSC method based on the concept of windowed energy, the integration horizon of which can be tuned to modify the energetic behavior of the stabilizer ranging from absolute energy domain stabilization up to absolute power domain stabilization. A windowed energy solution will not have the conservatism of the energy domain stabilizers suffering from infinite memory and will not be too sensitive to small changes in energy exchange dynamics, like power-domain stabilizers. This flexibility is in particular needed since the situation is more complex when the controller is designed to be compatible with non-passive environments. To provide more accurate analysis, let us consider a switching environment scenario as an example. A stabilizer developed in the energy domain is more conservative when the behavior of under observation source/sink of energy switches from non-passive to passive since the stabilizer continues to damp the energy for some time even after the system becomes passive. On the other hand, the power domain stabilizer is conservative when the opposite switch happens from passive to non-passive since it modulates the reflected force of every single power packet that does not satisfy the condition regardless of the memory of the interaction and the integral of passivity over time. Thus, unlike conventional methods, since the proposed VSPSC allows for both passive and non-passive environments, it is not possible to consider one of the two domains (energy versus power) as the least conservative or most effective. However, a more reasonable behavior of the stabilizer would be to have a tunable memory that forgets long term information and remembers recent interactional dynamics. This is realized for VSPSC for the first time in this paper based on a forgetting factor in the design of the stabilizer, as explained in the rest of the section.

Let us introduce the forgetting factor $0 \leq \Gamma \leq 1$ into the iterative integration function of Y(n) in (18), we will have:

$$Y(n) = \Gamma.Y(n-1) + \xi_p.v_p(n)^T.v_p(n) + \Gamma.f_{p_{mod}}(n-1)^T.v_p(n-1) \quad (19)$$

In (19), if $\Gamma = 1$, the formulation will converge to the energy domain, which is given in (18). If $\Gamma = 0$, the history will be forgotten, and Y(n) will be the (lower bound on the) power which can be damped by the biomechanics of the user at iteration "n". A moderate solution would be $0 < \Gamma < 1$ which encodes some finite memory in to the system. Combining (17) and (19) we have :

$$\psi_\Gamma = \Gamma.Y(n-1) + \xi_p.v_p(n)^T.v_p(n) + \Gamma.f_{p_{mod}}(n-1)^T.v_p(n-1) + f_{p_{mod}}(n)^T.v_p(n) \quad (20)$$

Thus as the controller (defined below) guarantees that $\psi_\Gamma > 0$ for a given positive Γ, we have $\psi > 0$, which means that the system is passive and hence stable. If $\Gamma = 0$, the controller will make every single interactional power packet positive to guarantee that the integral will be positive. In this case, the controller is acting as the power-domain discrete VSPSC. If $\Gamma = 1$, the result is energy-domain discrete VSPSC, and if $0 < \Gamma < 1$ the result is windowed energy discrete VSPSC.

To finalize the design of the windowed-energy stabilizer, based on the notes above it can be mentioned that the system is stable if :

$$\psi_\Gamma = Y(n) + f_{p_{mod}}(n)^T.v_p(n) \geq 0$$
$$\Rightarrow Y(n) + \gamma(n).f_p(n)^T.v_p(n) \geq 0$$
$$\Rightarrow \gamma(n) = \frac{-Y(n)}{f_p(n)^T.v_p(n)} \quad (21)$$

It should be noted that if $f_p(n).v_p(n) = 0$, then the synthesized γ may seem to be computationally singular. This phenomena has been seen in almost all passivity-based stabilizers [3]–[5], and is usually avoided by adding a small value of ϵ to the denominator when it is zero, to avoid such situation. This can be done here as well, but, it should be also noted that when $v_p = 0$, there is no power delivered, and we have $\xi_p.v_p(n)^T.v_p(n) + f_p(n).v_p(n) = 0$. As a result, the above problem can be easily mitigated by considering $\gamma = 1$. i.e. no force modification when $f_p(n).v_p(n) = 0$.

The γ calculated in (21) makes the energy zero even for passive interactions if it is always activated. Thus an activation mechanism should be taken into account to guarantee the stability of the system based on (21) while using γ only when needed. As a result, the Windowed-energy discrete VSPSC can be synthesized as follows.

Let $f_{R_G}(n) = \alpha.f_{p_{mod}}(n)$ and $f_{p_{mod}(n)} = \gamma_f(n).f_p(n)$, where α is the hyper parameter (with a default of unity) and $\gamma_f(n)$ is the adaptive force scaling parameter. Then to satisfy the stability condition, we have

$$\gamma_f(n) = \begin{cases} 1 & \text{if } Y(n) + f_p(n)^T.v_p(n) \geq 0 \\ 1 & \text{if } f_p(n)^T.v_p(n) = 0 \\ \frac{-Y(n)}{f_p(n)^T.v_p(n)} & \text{otherwise} \end{cases}$$

where,

$$Y(n) = \Gamma.Y(n-1) + \xi_p.v_p(n)^T.v_p(n) + \Gamma.f_{p_{mod}}(n-1)^T.v_p(n-1) \quad (22)$$

IV. Results

Here, we will simulate assistive and resistive virtual therapy for evaluation of the performance of the stabilizer for a wide range of delays and environment impedances through a grid study. The Z_h represents the impedance of the user's hand, and Z_e represents the therapeutic environment. Z_h was kept static in all experiments for consistency. For the purpose of the simulations, it is assumed that once the user-specific EoP map is generated, the estimate of EoP is 80% of the actual EoP. This is only to be distant from ideal condition in our simulation study. Since Z_h is assumed to be a pure damping of 50 N.s/m (and considering the fact that for mass-spring-damper systems, EoP is equal to the amount of damping), the conservative estimate of EoP is considered to be 40 N.s/m (80% of the actual value) in the simulations. The sinusoidal exogenous force of $Sin(10t) + Cos(5t)$ is applied by the patient while the therapist applies no exogenous forces (except for the first simulation) while showing a power-assistive/resistive behavior.

A. Discrete Windowed VSPSC vs TDPA

• **Velocity and Force Profiles**: The velocity and force plots for Discrete Windowed VSPSC and TDPA are provided in the Fig. 4 and 5. Fig. 4 corresponds to a teleoperation system with no delay while for Fig. 5, a relatively-large and variable time delay of $300 + 60Sin(20t)$ milliseconds was considered. The top 3 plots in both figures correspond to discrete Windowed VSPSC for forgetting factors of 1, 0.99 997, and 0, respectively. The last plot corresponds to the energy domain TDPA (the conventional

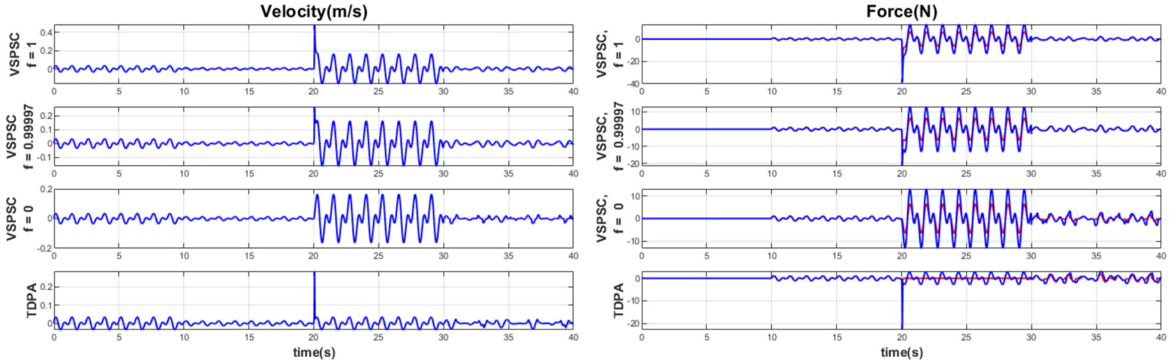

Fig. 4. Velocity and Force for (a) VSPSC with forgetting factor: 0, 0.99 997, 1, and (b) Energy Domain TDPA. No time delay.

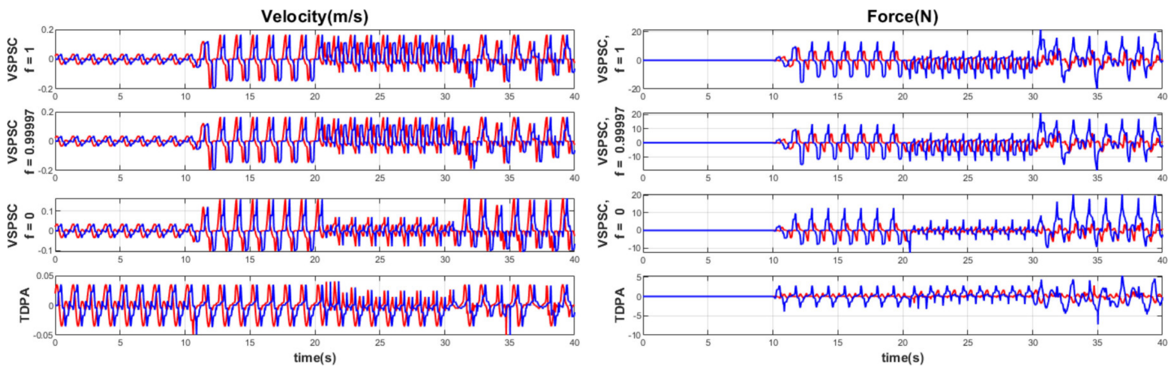

Fig. 5. Velocity and Force for (a) VSPSC, and (b) Energy Domain TDPA. Variable time delay of $300 + 60Sin(20t)ms$.

technique, for comparison). The plots are divided into 4 phases: (a) The first 10 seconds correspond to no force applied by the therapist, which results in free motion of the robot at the patient side; (b) The time ranges of [10,20) seconds are resistive therapy with therapist impedance (Z_e) of $+80Ns/m$; (c) Between 20 and 30 seconds assistive therapy with therapist impedance of $-80Ns/m$ was considered; (d) The next 10 seconds (i.e., [30,40) seconds) corresponds to resistive therapy with added inertia and stiffness components to the therapist's behavior with the values of $1\,kg$ and $300\,N/m$, respectively, along with the damping coefficient of 80 Ns/m. In addition, an exogenous force of $Sin(5t) + 2Cos(8t)$ is applied by the therapist. The exogenous force of $Sin(10t) + Cos(5t)$ was applied by the patient since the beginning of the experiment.

For no delay profile, the results are shown in Fig. 4. As can be seen, using both the proposed VSPSC and the conventional TDPA, the velocity profiles are perfectly tracking throughout the experiments. Also, during the resistive phases of (b) and (d), force tracking is almost perfect for all controllers. The proposed VSPSC approach, using the forgetting factor of 1 and 0.99 997, performed better (less error) in terms of force tracking during resistive Phase (d) when almost perfect force tracking is achieved. However, the conventional TDPA showed considerable errors in force tracking of Phase (d) even when the delay was zero. This is due to the injected energy by the exogenous force of the therapist during this Phase, which cannot be handled properly using the conventional approach. More importantly, during the assistive Phase of the therapy (i.e., Phase (c)), the conventional TDPA controller failed to deliver any force packets, and it flattened all the delivered forces completely due to the non-passive nature of assistive therapy in Phase (c). This highlights the inability of the conventional technique in handling assistive cases. However, the proposed VSPSC controller using all the three forgetting/windowing factors was able to deliver a large amount of force in assistive Phase C, taking advantage of novel features of the proposed approach. This shows the superior behavior of the proposed technique when compared to the conventional method. It should also be highlighted that at time t = 20 seconds when the simulation switches from assistive to resistive therapy, a significant overshoot occurs in the behavior of the conventional controller, nearly five times larger than the normal amplitude of the trajectory. This can result in major safety concerns in practice. It can be seen that a much smaller overshoot exists when the forgetting/windowing factor of 1 is considered for the proposed VSPSC. And the overshoot is totally eliminated for the other two choices of forgetting/windowing factor of the proposed VSPSC. This again shows the superiority of the proposed technique. When the variable delay is present in the communication channel as shown in Fig. 5, the proposed stabilizer additionally compensates for the instability induced by the delay during both resistive and assistive therapies in addition to the active excess energy induced by the therapist. It is clearly visible in the figures that even upon addition of inertial and stiffness components to the therapist impedance as well as the application of external exogenous (active) forces by the therapist (between the time range of [30, 40) seconds), the DWE-VSPSC

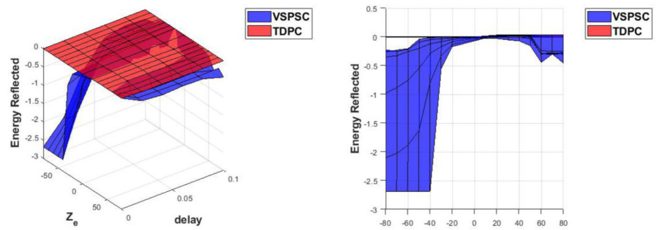

Fig. 6. Reflected Energy from Therapist to the Patient Side.

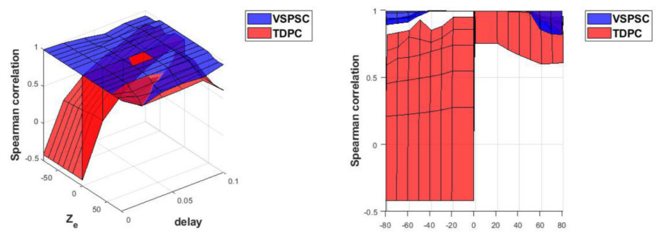

Fig. 7. Spearman Correlation between $f_{p_{mod}}$ and f_p .

is able to stabilize the system while also taking into account the EOP of the user's (patient's) biomechanics and outperforms the TDPA.

• **Energy Reflection Factor and Spearman Correlation**: Figures Fig. 6 and Fig. 7 show plots comparing DWE-VSPSC ($\Gamma = 1$) and Energy Domain TDPA. For this purpose, the energy reflection factor is calculated as, $E_{reflect} = \int_0^t f_{p-mod}^T.v_p.d\tau$. Fig. 6(a) displays a 3D plot for energy reflection factor from the therapist to the patient with respect to power amplification/dissipation, using a range of $Z_e \in [-80\,N.s/m, 80\,N.s/m]$ and a range of delay $\in [0, 100ms]$. Fig. 6(a) is the corresponding side-view with respect to Z_e. It can clearly be seen that DWE-VSPSC allows for the flow of energy for both assistive and resistive scenarios and modifies that depending on the energy absorption capacity of the users. In contrast, TDPA completely blocks the flow of energy when non-passivity is detected.

Fig. 7(a) displays a 3D plot for Spearman correlation which indicates the nonlinear and nonparametric relationship between force at the therapist side (f_e) and the force reflected to the patient ($f_{p_{mod}}$), when Z_e belongs to $[-80, 80]$ and delay belongs to $[0, 100ms]$. Fig. 7(b) is the corresponding side view w.r.t Z_e. This correlation factor is close to 1 for VSPSC indicating that VSPSC maintains a close monotonic relationship between the $f_{p_{mod}}$ and f_e for any Z_e (resistive and assistive cases). The correlation is much worse for TDPA in case of assistive therapy since it completely blocks the energy reflection. Even in resistive case, the correlation values for VSPSC are superior when compared with TDPA which indicates that VSPSC outperforms TDPA.

B. Comparing Different Forgetting Factors

• **Case 1: Reflected Impedance**: The reflected impedance represents the extent of the assistive/resistive therapy delivered from the therapist (environment) to the patient, in the telerobotic system [2]. It is calculated as,

$$D_{reflect} = \frac{\int_0^t f_{p-mod}^T.v_p.d\tau}{\int_0^t v_p^T.v_p}. \tag{23}$$

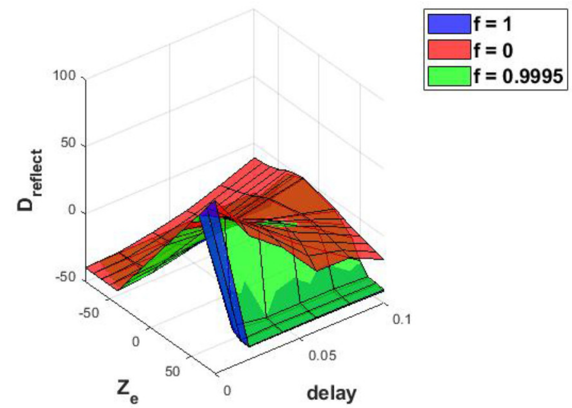

Fig. 8. Reflected Impedance.

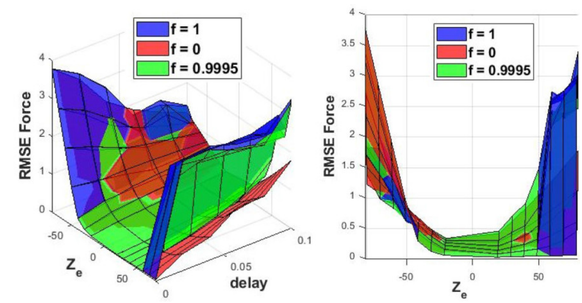

Fig. 9. RMSE of Force Modification.

Fig. 8 displays the reflected impedance over a range of $Z_e \in [-80Ns/m, +80Ns/m]$ for forgetting factors (Γ) of 1 (i.e., DE-VSPSC, in blue), 0 (i.e., Discrete Power-domain VSPSC, in red) and 0.9995 (i.e., DWE-VSPSC, in green). For an ultimately transparent system, the reflected impedance must be equal to the impedance provided by the therapist. However, in the presence of delay and assistive therapy, parts of non-passive energy that may cause instability should be modified, affecting the reflected impedance. Since in the simulation we consider the estimate of EOP to be $40\,N.s/m$, it can be seen that $D_{reflect}$ gets saturated at -40 N.s/m during the assistive part, which shows that all three forgetting factor for the proposed stabilizer are able to reflect the non-passive impedance considering the EoP of the biomechanics. As can be seen in Fig. 8 when there is no delay, the response of the three forgetting factors is relatively similar. For large delays, the behaviors of the three forgetting factors are different, securing different degrees of conservatism, as explained before.

• **Case 2: RMSE of Force Modification**: The root mean square error (RMSE) between the force generated by the environment (therapist) and the force that is reflected for the user after modification by the stabilizer is studied here. The results are given in Fig 9 for 3 values of forgetting factors against different delay values ($delay \in [0, 100ms]$ and impedances ($Z_e \in [-80, 80]$). It can be seen that smaller forgetting factors perform better for larger delays during resistive therapies, while for assistive therapies, the higher values of forgetting factors generally perform better. This shows the tunable behavior of the proposed family of stabilizer using the concept of windowed energy.

V. Conclusion and Future Works

In this paper, a novel adaptive stabilization framework was proposed, which can be used for many telerobotic, haptics, and human-centered robotic systems. The particular application is considered to be telerobotic rehabilitation. The proposed scheme is capable of exploiting the passivity signature of the user's biomechanics during physical interaction with robots to reduce the conservatism and allow for the non-passive energy to flow, which is an imperative need, especially for assistive systems. The stabilizer is named Discrete Windowed Energy Variable Structure Passivity Signature Control (DWE-VSPSC). The concept of windowed energy was combined with the proposed design, for the first time, to allow for tuning the behavior of the stabilizer and introducing a family of stabilization schemes that can range from purely power-domain to purely energy-domain stabilization. The proposed approach also removed the dependency on the sampling time, which exists in state-of-the-art passivity stabilization techniques. Also, the proposed approach utilizes adaptive force scaling instead of adaptive damping to reduce the complexity of topology. Novel theoretical developments and stability proof were given. To evaluate the performance, a wide range of simulations have been conducted in a systematic manner under various delay and impedance conditions. The performance was compared with an existing state-of-the-art algorithm. We have shown that VSPSC outperforms the existing stabilization scheme while relaxing any assumption on the passivity of the environment and while being compatible with variable network delays (without any restriction on the rate of change of delay). It should be noted that the proposed framework reduces the conservatism of physical-human robot interaction by exploiting any estimate of EoP. The higher the accuracy of the estimate, the better the performance.

The future work of this paper focuses on addressing the existing limitations of the paper. In this regard, we will (a) conduct experimental validation of VSPSC to compare the performance of the proposed stabilizer with respect to the existing solutions in the literature through experimental implementation, (b) find the optimal value of the windowing factor to further enhance the performance, and (c) evaluate the potential effect of biomechanical parameters. Thus, besides the grasping pressure, other parameters such as kinematics will be investigated to further enhance the estimate of EoP and augment the performance of the stabilizer.

References

[1] R. J. Anderson and M. W. Spong, "Bilateral control of teleoperators with time delay," *IEEE Trans. Autom. control*, vol. 34, no. 5, pp. 494–501, May 1989.

[2] S. F. Atashzar *et al.*, "A small-gain approach for nonpassive bilateral telerobotic rehabilitation: Stability analysis and controller synthesis," *IEEE Trans. Robot.*, vol. 33, no. 1, pp. 49–66, Feb. 2017.

[3] J.-H. Ryu *et al.*, "A passive bilateral control scheme for a teleoperator with time-varying communication delay," *Mechatronics*, vol. 20, no. 7, pp. 812–823, 2010.

[4] V. Chawda and M. K. O'Malley, "Position synchronization in bilateral teleoperation under time-varying communication delays," *IEEE/ASME Trans. Mechatronics*, vol. 20, no. 1, pp. 245–253, Feb. 2015.

[5] M. Shahbazi *et al.*, "Position-force domain passivity of the human arm in telerobotic systems," *IEEE/ASME Trans. Mechatronics*, vol. 23, no. 2, pp. 552–562, Apr. 2018.

[6] S. F. Atashzar *et al.*, "A grasp-based passivity signature for haptics-enabled human-robot interaction: Application to design of a new safety mechanism for robotic rehabilitation," *Int. J. Robot. Res.*, vol. 36, no. 5-7, pp. 778–799, 2017.

[7] S. F. Atashzar *et al.*, "A new passivity-based control technique for safe patient-robot interaction in haptics-enabled rehabilitation systems," in *Proc. IEEE/RSJ Int. Conf. Intell. Robots Syst.*, 2015, pp. 4556–4561.

[8] S. F. Atashzar *et al.*, "A passivity-based approach for stable patient-robot interaction in haptics-enabled rehabilitation systems: Modulated time-domain passivity control," *IEEE Trans. Control Syst. Technol.*, vol. 25, no. 3, pp. 991–1006, May 2017.

[9] S. F. Atashzar *et al.*, "Control of time-delayed telerobotic systems with flexible-link slave manipulators," in *Proc. IEEE/RSJ Int. Conf. Intell. Robots Syst.*, 2012, pp. 3035–3040.

[10] G. Niemeyer and J.-J. Slotine, "Stable adaptive teleoperation," *IEEE J. Ocean. Eng.*, vol. 16, no. 1, pp. 152–162, Jan. 1991.

[11] Jee-Hwan Ryu *et al.*, "Stable teleoperation with time domain passivity control," in *Proc. IEEE Int. Conf. Robot. Automat.*, vol. 3, 2002, pp. 3260–3265.

[12] J.-H. Ryu *et al.*, "Stable teleoperation with time-domain passivity control," *IEEE Trans. Robot. Automat.*, vol. 20, no. 2, pp. 365–373, Apr. 2004.

[13] F. Ferraguti *et al.*, "Optimized power modulation in wave based bilateral teleoperation," *IEEE/ASME Trans. Mechatronics*, vol. 26, no. 1, pp. 276–287, Feb. 2021.

[14] M. Laghi *et al.*, "Unifying bilateral teleoperation and tele-impedance for enhanced user experience," *Int. J. Robot. Res.*, vol. 39, no. 4, pp. 514–539, 2020.

[15] D. Heck *et al.*, "Direct force-reflecting two-layer approach for passive bilateral teleoperation with time delays," *IEEE Trans. Robot.*, vol. 34, no. 1, pp. 194–206, Feb. 2018.

[16] D. Sun *et al.*, "Neural network-based passivity control of teleoperation system under time-varying delays," *IEEE Trans. Cybern.*, vol. 47, no. 7, pp. 1666–1680, Jul. 2017.

[17] D. Sun *et al.*, "Wave-variable-based passivity control of four-channel nonlinear bilateral teleoperation system under time delays," *IEEE/ASME Trans. Mechatronics*, vol. 21, no. 1, pp. 238–253, Feb. 2016.

[18] S. F. Atashzar *et al.*, "Networked teleoperation with non-passive environment: Application to tele-rehabilitation," in *Proc. IEEE/RSJ Int. Conf. Intell. Robots Syst.*, 2012, pp. 5125–5130.

[19] S. F. Atashzar *et al.*, "Energetic passivity decoding of human hip joint for physical human-robot interaction," *IEEE Robot. Automat. Lett.*, vol. 5, no. 4, pp. 5953–5960, Oct. 2020.

[20] M. Vidyasagar, *Nonlinear Systems Analysis.*, Society for Industrial and Applied Mathematics, 2002.

[21] J. R. Forbes and C. J. Damaren, "Passive linear time-varying systems: State-space realizations, stability in feedback, and controller synthesis," in *Proc. Amer. Control Conf.*, 2010, pp. 1097–1104.

[22] H. K. Khalil and J. W. Grizzle, Nonlinear systems, Upper Saddle River, NJ: Prentice hall, vol. 3, 2002.

[23] S. M. Hatem *et al.*, "Rehabilitation of motor function after stroke: A multiple systematic review focused on techniques to stimulate upper extremity recovery," *Front. Hum. Neurosci.*, vol. 10, p. 442, 2016.